Structures of Rare Earth Homodinuclear Macrocyclic Complexes with the Polyamine Polycarboxylic Ligand 1,4,7,10,14,17,20,23-Octaazacyclohexacosane-1,4,7,10,14,17,20,23-octaacetic Acid (H_8OHEC) in the Crystal and in Solution

Herbert Schumann,*[a] Ulrike A. Böttger,[a] Hardy Weisshoff,*[b] Burkhard Ziemer,[b] and Adolf Zschunke[b,c]

Dedicated to Professor Dr. Manfred Meisel on the occasion of his 60th birthday

Keywords: Crystal structure / Solution structure / Homodinuclear lanthanide complexes / Lanthanides / Macrocyclic ligands / Polyamine polycarboxylic acid

The solid-state structures of the four homodinuclear chelate complexes, $[Na_2(Y_2OHEC)(H_2O)_2] \cdot 7\ H_2O \cdot C_2H_5OH$ (**1**), $[Na_2(Gd_2OHEC)(H_2O)_2] \cdot 12\ H_2O$ (**2**), $[Na_2(Eu_2OHEC)(H_2O)_2] \cdot 11\ H_2O$ (**3**), and $[Cs_2(La_2OHEC)(H_2O)_2] \cdot 14\ H_2O$ (**4**) (H_8OHEC = 1,4,7,10,14,17,20,23-octaazacyclohexacosane-1,4,7,10,14,17,20,23-octaacetic acid), were determined by X-ray crystal structure analysis. Each lanthanide(III) ion is ninefold coordinated by eight donor atoms of the ligand system and the oxygen atom of one water molecule. The structures are compared with those of DOTA- and TETA-coordinated complexes and the conformation of the OHEC ligand system with that of the parent amine and its dinuclear copper complex. NMR investigations of the diamagnetic complex **1** indicate a very similar environment of the lanthanide cations in solution and in the solid state. Low-temperature and variable-temperature ^{1}H-NMR measurements prove the existence of two isomers of **1** (3.5:1 ratio) which undergo conformational processes. The rate constants of these processes were deduced from a complete line shape analysis and were used to determine the activation parameters.

Introduction

Lanthanide complexes with macrocyclic polyamine polycarboxylate ligand systems have been the subject of many investigations[1] because they are promising substances for biomedical applications in the field of radioimmunotherapy[2] and can be used as contrast-enhancing agents in magnetic resonance imaging.[3] The best investigated compounds of this class are the mononuclear lanthanide(III) chelates of the macrocyclic ligand DOTA (1,4,7,10-tetraazacyclododecane-1,4,7,10-tetraacetate) and of ligands based on the DOTA skeleton.[4,5] The solid state X-ray structures of DOTA complexes of Ln^{III} (Ln= Y,[4d] La,[4f] Eu,[4a] Gd,[4b,c] and Lu[4e]) show the metal ions in a mono-capped square-antiprismatic coordination sphere. The high rigidity of the DOTA complexes allowed the estimation of conformational and coordination equilibria in aqueous solution by NMR spectroscopy.[4e,6]

In contrast, only a few binuclear lanthanide(III) complexes with macrocyclic polyamine ligands are known, e.g. Eu^{III}, Gd^{III}, and Tb^{III} complexes of a branched hexaazacyclododecane ligand containing six 2,2′-bipyridine pendants units,[7] Gd^{III} complexes of DOTA derivatives in which the two metal ions are located between two ligand molecules forming a dimeric unit,[5d] and the complex $[BO\{Gd(DO3A)(H_2O)\}_2]$ in which the two DO3A rings $\{BO(DO3A)_2$ = 2,11-dihydroxy-4,9-dioxa-1,12-bis[1,4,7,10-tetraaza-4,7,10-tris(carboxymethyl)cyclododecyl]dodecane$\}$ are connected by a dihydroxydioxadodecane chain.[8]

Recently we reported the successful synthesis of two new hexadecadentate macrocyclic polyamine polycarboxylic ligands H_8OTEC (1,4,7,10,13,16,19,22-octaazacyclotetracosane-1,4,7,10,13,16,19,22-octaacetic acid) and H_8OHEC (1,4,7,10,14,17,20,23-octaazacyclohexacosane-1,4,7,10,14,17,20,23-octaacetic acid) and of some of their mono- and dinuclear lanthanide(III) chelate complexes,[9] among them the binuclear OHEC complexes of Y, Gd, and Eu. The acid/base properties of these ligands were characterised by potentiometry and NMR titration techniques.[10]

In this paper we present the crystal structures of the homodinuclear complexes of yttrium(III), gadolinium(III), europium(III), and lanthanum(III) with the ligand H_8OHEC as well as the solution structure and the dynamics of the diamagnetic Y^{III} complex.

---

[a] Institut für Anorganische und Analytische Chemie,
Technische Universität Berlin,
Strasse des 17. Juni 135, D-10623 Berlin, Germany
Fax: (internat.) +49 (0)30/3142 2168
E-Mail: schumann@chem.tu-berlin.de

[b] Institut für Angewandte Analytik und Umweltchemie,
Humboldt Universität zu Berlin,
Hessische Str. 1−2, D-10115 Berlin, Germany

[c] Bundesanstalt für Materialforschung und -prüfung,
Rudower Chaussee 5, D-12489 Berlin, Germany

💻 Supporting information for this article is available on the WWW under http://www.wiley-vch.de/home/eurjic or from the author.

Results and Discussion

Synthesis

The homodinuclear lanthanide(III) complexes were synthesised by treating H_8OHEC with the lanthanide oxides Ln_2O_3 (Ln = Eu,[9] Gd,[9] La) in refluxing water. Freshly prepared $Y(OH)_3$[9] was used for the synthesis of the yttrium complex instead of Y_2O_3, because of the faster reaction in that case. The colourless and highly water-soluble complexes were characterised by means of FAB-MS.

$$2\ Y(OH)_3 + H_8OHEC + 2\ NaOH \rightarrow Na_2[Y_2(OHEC)(H_2O)_2] + 6\ H_2O$$

1

$$Ln_2O_3 + H_8OHEC + 2\ MOH \rightarrow M_2[Ln_2(OHEC)(H_2O)_2] + 3\ H_2O$$

2 (Ln/M = Gd/Na),
3 (Ln/M = Eu/Na),
4 (Ln/M = La/Cs)

As known from the synthesis of the DOTA and modified DOTA lanthanide(III) complexes,[6a,11,12] the formation of the compounds **1** to **4** is also slow. A pH value of 8.5 and heating of the aqueous solutions to reflux are essential reaction conditions for the entrance of the lanthanide ions into the tetraaza coordination pockets of the OHEC ligand, which otherwise would be blocked by protonation of the strongly basic ring nitrogens. This is supported by the protonation scheme of H_8OHEC established by potentiometric titration and pH-dependent $^1H/^{13}C$ NMR titration [the four highest protonation constants were assigned to the ring nitrogens: log K = 11.07, 10.21, 9.58, and 8.54 (298 K, 0.1 M KCl)].[10] In neutral or acidic solution, the lanthanide ions are coordinated only weakly to the outer sphere of the cyclic ligand[13] and free lanthanide ions can be detected electrochemically,[14] by ^{89}Y-NMR,[9] and by reaction with xylenol orange.

Molecular Structures

The molecular structures of the complexes **1** to **4** were determined by single crystal X-ray diffraction. Suitable single crystals were obtained from saturated aqueous solutions of the pure complexes either by slow diffusion of ethanol into the solution of **1** or by slow evaporation of the solutions of **2**, **3**, or **4**. The composition of the crystals correspond to the formulas $[Na_2(Y_2OHEC)(H_2O)_2] \cdot C_2H_5OH \cdot 7\ H_2O$ (**1**), $[Na_2(Gd_2OHEC)(H_2O)_2] \cdot 12\ H_2O$ (**2**), $[Na_2(Eu_2OHEC)(H_2O)_2] \cdot 11\ H_2O$ (**3**) or $[Cs_2(La_2OHEC)(H_2O)_2] \cdot 14\ H_2O$ (**4**). All four complexes crystallise in the monoclinic space group $P2_1/n$. The crystal data, the data collection and the refinement parameters are listed in Table 4 (see Experimental Section).

Although only the Gd^{III} complex **2** and the Eu^{III} complex **3** are isostructural, the conformation of the macrocyclic OHEC unit as well as the coordination geometry around the metal ions are the same for all four structures. Figures 1a and 1b show the solid conformation of **1** in two different views for better understanding, Figure 1c shows the conformation in $[Na(YDOTA)(H_2O)]$ to visualise the differences of the acetate and the amine coordination in complexes of lanthanide metals with DOTA and OHEC. Due to the different ionic radii of the metals, the structures differ in the positions of the lanthanide ions with respect to the mean plane of the cyclic ligand. Whereas in the Y^{III} and La^{III} complexes **1** and **4** the inversion centre of the space group $P\ 2_1/n$ corresponds to the centre of gravity of the molecule resulting in a centrosymmetric geometry, the two halves of the molecules **2** and **3** containing the Gd^{III} and Eu^{III} ions are only almost equal to each other.

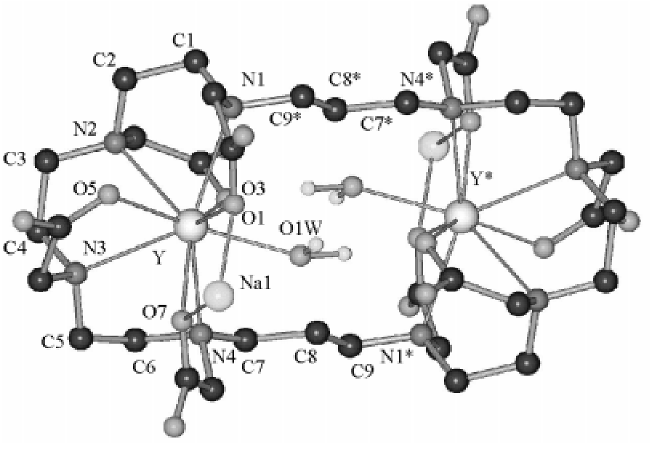

Figure 1a. Solid-state conformation of **1** with numbering scheme; with * designated atoms represent symmetry-equivalent positions ($-x$, $-y$, $-z$); for selected bond length [pm] and angles [°] in **1** see Supporting Information

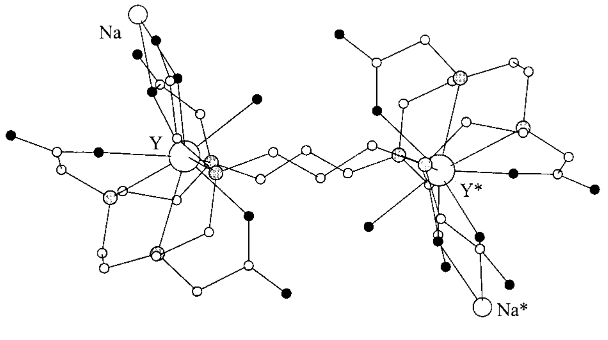

Figure 1b. Solid-state conformation of **1**, side view; carbon atoms contours only, nitrogen atoms filled grey, oxygen atoms filled black

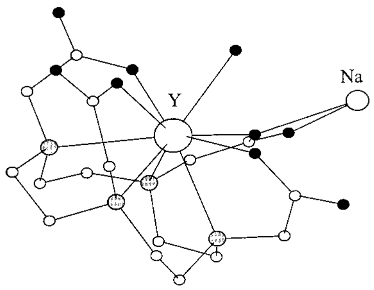

Figure 1c. Solid-state conformation of $[Na(YDOTA)(H_2O)]$; carbon atoms contours only, nitrogen atoms shaded in grey, oxygen atoms black

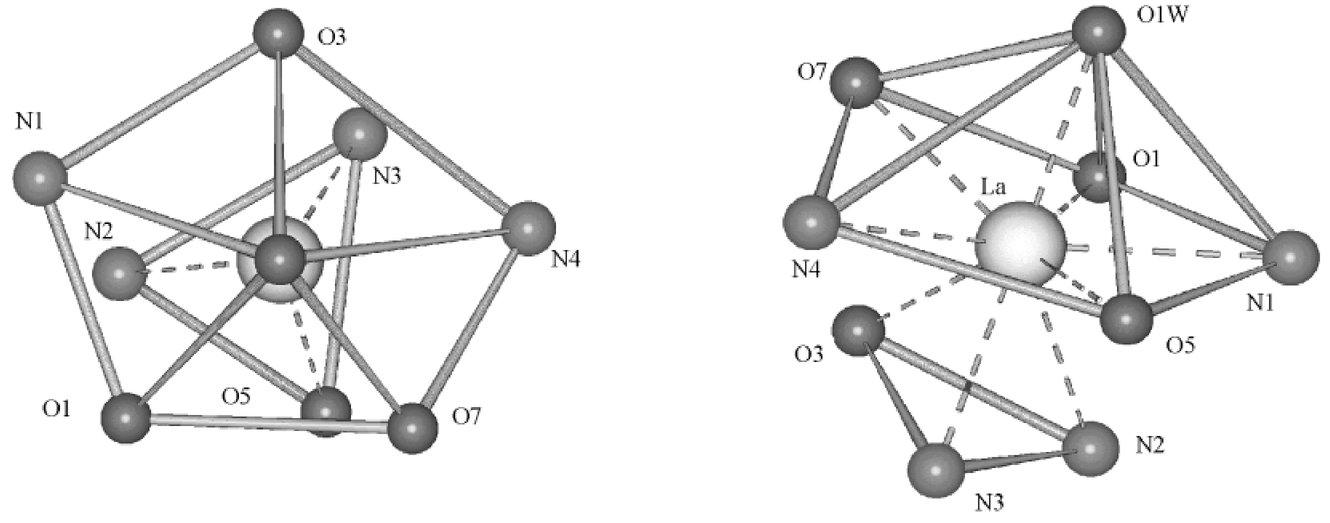

O1W−La−N4	76.11(19)	O7−La−N4	62.77(18)	N3−La−N2	66.49(2)
O1W−La−N2	144.60(2)	O3−La−N4	70.97(19)	N1−La−N2	66.39(19)
O1W−La−N3	140.30(2)	O3−La−N1	83.43(18)	N3−La−N4	67.47(19)
O1W−La−N1	92.10(2)	O1−La−N1	62.22(18)	O7−La−O1	79.30(18)
O1W−La−O1	68.39(18)	O3−La−N2	62.90(2)	O3−La−O1	136.11(19)
O5−La−O1W	135.07(19)	O7−La−N3	70.30(2)	O5−La−O1	69.48(18)

Figure 2. Coordination polyhedron about the lanthanum ion in **4**, top view (left) and side view (right); angles [°] involving lanthanum(III) and atoms from the coordination sphere

Coordination Geometry of the Lanthanide Ions

As demonstrated for **1** in Figure 1, the two lanthanide ions of each complex are completely encapsulated by the macrocyclic ligand. Each lanthanide ion is coordinated by the four nitrogen and four carboxylic oxygen atoms belonging to one half of the overall hexadecadentate ligand. The ninth coordination site of each lanthanide ion is occupied by the oxygen atom of a water molecule. However, the resulting coordination geometry corresponds neither to a monocapped square antiprism, nor to a tricapped trigonal prism, the two coordination polyhedrons representing the most common geometries of nine-coordinate complexes.[15] It can be best described in terms of an irregular polyhedron built up by a trigonal plane and a monocapped pentagonal plane (Figure 2). Three oxygen atoms and two nitrogen atoms of the ligand form the pentagonal plane [the maximum deviation of the atoms from this plane is observed in **2** (22 pm)], which is capped by the oxygen atom of a water molecule. The donor atoms remaining from this half of the ligand, one carboxylic oxygen and two nitrogen atoms, form the trigonal plane. The lanthanide ion is sandwiched between these two planes with a shorter distance to the centre of the capped pentagonal plane (for $\mathrm{Gd^{III}}$ in **2** the distance from the pentagonal plane is 46 pm, that from the trigonal plane is 195 pm). In all complexes, the capping oxygen atom of the water molecule and the lanthanide ion lie on an axis passing through the centres of both planes.

In contrast to the DOTA-like lanthanide complexes, in which all acetate groups are situated on one side of the ring adopting a four-bladed propeller-like conformation (see Figure 1c), three of the four carboxylic groups of the OHEC ligand coordinate each lanthanide(III) ion from one side of the ligand ring and the fourth from the opposite side (see Figure 1b).

A least-square plane of the macrocycle formed from the propylene chains and the four adjacent N atoms was calculated for all four complexes. The displacement of the lanthanides from this plane increases with increasing ionic radius of the lanthanide. For the $\mathrm{La^{III}}$ complex **4**, the least-squares equation for this plane, defined by the atoms C7, C8, C9, N4, and N1 and the corresponding symmetry-equivalent atoms, corresponds to $-9.5290x + 8.9063y + 3.1741z - 1.5870 = 0$. The maximum deviation of the carbon atoms from this plane is −38.41 pm, that of the nitrogen atoms −19.76 pm. The $\mathrm{La^{III}}$ ions are found ±37.47 pm centrosymmetrically above and below this mean plane. The displacement of the other lanthanide atoms from the corresponding ring mean planes is ±33.06 pm for $\mathrm{Y^{III}}$ in **1**, +36.53 pm and −31.76 pm for $\mathrm{Gd^{III}}$ in **2** and +35.20 pm and −32.30 pm for $\mathrm{Eu^{III}}$ in **3**.

Like the metal ions, the metal-coordinating water molecules are situated centrosymmetrically (**1**, **4**) or nearly centrosymmetrically (**2**, **3**) above and below the mean ring planes with Ln−O(water) distances in the range of the Ln−O(acetate) distances (Table 1). The $\mathrm{Gd^{III}{-}OH_2}$ contacts are similar to those found for mononuclear complexes.[4b,c;5a,e]

The minimum and maximum bond angles and interatomic distances of the OHEC ligand (Table 1) agree quite well with those found for TETA (1,4,8,11-tetraazacyclotetradecane-1,4,8,11-tetraacetate)[4g] and DOTA polyaza polycarboxylic complexes.[4] Moreover, the Ln−N and Ln−O contacts are within the range of the values reported for mononuclear structures.[4] The differences between the maximum and minimum interatomic distances are greatest for Ln−O in **1** and for Ln−N in **3**, whereas the smallest differences are found for **4**, but altogether, all these differences are much smaller than those reported for the ion $[Eu(DOTA)(H_2O)]^-$, the complex with the greatest distortions within the series of DOTA lanthanide complexes.[4a]

Conformation of the Ligand

The overall conformation of the OHEC macrocycle in the diyttrium complex **1** is shown in Figure 3, together with the qualitative torsion angles. To accommodate two large lanthanide(III) ions within the ring a centrosymmetric biangular conformation, label {13 13} by Dale,[16] with two genuine corners is adopted, which allows all eight nitrogen atoms to direct their lone electron pair efficiently to the lanthanide ions. The fourfold repetition of *anti* torsion angles in the propylene chains expands the ring. This conformation was found to be essentially the same in all four complexes (for torsion angles of the macrocycle in the dilanthanide(III) OHEC complexes see Supporting Information).

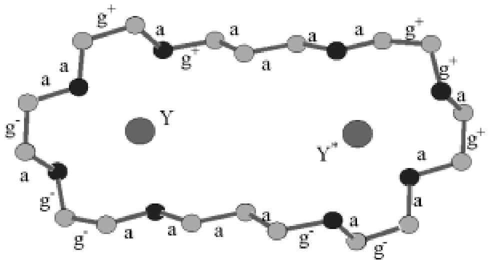

Figure 3. Conformation of the OHEC-ligand in **1**, with corresponding qualitative torsion angles

Surprisingly, the uncomplexed macrocycle of the parent compound OHEC-amine (1,4,7,10,14,17,20,23-octaazacyclohexacosane)[9] shows a highly ordered conformation ruled by a hydrogen-bonding pattern. Its solid state structure reveals a centrosymmetric quadrangular {10 3 10 3} conformation, established by both intramolecular and intermolecular three-centre and two-centre NH···N interactions, thus preventing the enclosure of water molecules into the crystal. This conformation represents a preorganised state for small transition metal ions. In fact, the OHEC-

Table 1. Minimum and maximum interatomic distances [pm] and angles [°] in dilanthanide(III) OHEC complexes and related compounds

	1	**2**	**3**	**4**	**$[Eu(DOTA)]^-$** [4a]	**$[Tb(TETA)]^-$** [4g]
C−C	150.5(6) 152.8(5)	150.5(6) 152.5(6)	149.4(9) 153.1(9)	154.4(10) 150.0(11)	162.3(6) 142.6(5)	149.4(5) 154.8(6)
C−N	147.9(5) 150.8(5)	149.9(5) 146.8(5)	146.9(8) 150.1(9)	150.8(10) 146.3(10)	164.3(6) 137.5(4)	147.4(5) 150.9(5)
C−O	128.4(5) 124.9(5)	128.9(5) 125.8(5)	123.1(10) 125.4(8)	127.9(10) 125.6(10)	120.2(5) 139.0(5)	123.6(5) 124.2(5)
C=O	122.4(5) 125.7(5)	125.2(5) 122.3(6)	127.8(8) 126.0(8)	122.2(10) 125.0(9)	116.1(5) 132.5(5)	125.4(5) 128.7(5)
C−C−C	106.5(3)	106.0(3) 108.2(3)	106.8(5) 108.4(5)	106.2(6)		
C−N−C	103.3(3) 111.0(3)	103.6(3) 110.1(3)	103.9(5) 110.8(5)	103.9(6) 110.9(6)	104.6(3) 114.6(3)	106.1(3) 110.4(3)
N−C−C	110.7(3) 118.4(3)	110.1(3) 118.0(3)	111.5(6) 118.3(5)	106.2(6) 117.8(6)	107.0(3) 117.1(3)	110.3(3) 116.2(3)
O−C−O	124.3(4) 125.2(4)	123.4(5) 125.4(4)	123.0(7) 126.2(6)	122.3(8) 125.7(8)	116.9(4) 130.5(3)	123.5(4) 125.8(4)
O−C−C	116.6(3) 118.9(4)	116.9(3) 118.7(4)	117.2(6) 118.8(6)	117.6(7) 118.4(7)	112.4(4) 117.0(3)	117.5(4) 118.0(4)
O^M−C−C	115.9(4) 118.2(3)	116.6(4) 118.6(4)	116.4(6) 118.6(4)	117.0(7) 118.4(7)	112.5(4) 120.8(3)	117.1(3) 117.8(3)
Ln−O	241.2(2) 228.4(3)	234.7(3) 246.5(3)	236.2(4) 248.2(4)	246.4(5) 252.9(5)	251.1(3) 238.7(3)	230.2(3) 233.0(3)
Ln−N	264.7(3) 276.7(3)	262.3(4) 276.7(4)	265.4(5) 279.9(5)	275.3(6) 286.7(6)	290.0(3) 251.0(3)	257.5(3) 262.0(3)
$Ln-OH_2$	236.3(3)	240.6(3) 243.8(3)	243.0(5) 246.0(5)	252.6(6)	248.0(3)	
Ln−Ln	665.3	652.1	652.0	636.0		
O−Ln−O	74.46(9) 133.97(9)	74.13(15) 134.73(15)	73.84(10) 135.11(10)	79.30(18) 133.70(18)	78.46(9) 147.51(9)	74.1(1) 133.46(9)
O−Ln−N	64.93(9) 139.38(9)	64.27(15) 138.34(16)	64.78(10) 138.56(10)	62.22(18) 140.82(18)	60.79(9) 143.63(9)	66.63(9) 151.50(9)
N−Ln−N	67.43(11) 145.79(9)	67.65(17) 149.19(16)	67.70(11) 148.26(10)	66.40(2) 151.99(19)	64.69(9) 107.56(9)	70.4(1) 136.74(9)
O−Ln−OW	66.88(10) 135.61(10)	67.25(15) 135.19(15)	67.16(10) 135.31(11)	68.39(18) 135.07(19)	68.67(9) 75.58(9)	
N−Ln−OW	76.51(10) 141.55(12)	77.92(16) 140.45(17)	77.68(11) 40.65(12)	76.11(19) 144.6(2)	124.5(1) 129.81(9)	

amine ligand of the dinuclear Cu^{II} complex [Cu$_2$(OHEC-amine)(SO$_4$)$_2$][9] adopts in the solid state a very similar {5 5 3 5 5 3} conformation (for torsion angles of the macrocycle in the OHEC-amine ligand and in [Cu$_2$(OHEC-amine)(SO$_4$)$_2$] see Supporting Information).

Packing Pattern

All four complexes are wrapped in a water matrix. Besides the water molecules coordinated to the metal ions, the complexes **2** to **4** contain 12, 11, or 14 additional water molecules, respectively. In **1**, the position of one water molecule is occupied to 50% by ethanol, with identical positions of the oxygen atoms.

The crystal of **1** is built up from infinite one-dimensional chains of [Y$_2$(OHEC)(H$_2$O)$_2$]$^{2-}$ units, arranged parallel to the *a* axis and linked by a network of Na$^+\cdots$O contacts, involving the sodium cation, the carboxylate oxygen atoms and the water molecules associated with the cation. In **2** and **3** the chain runs along the *c* axis. The molecular units of **4** are held together by caesium ions and water molecules forming an infinite chain parallel to the *a* axis. In all structures there is an additional three-dimensional framework built up by hydrogen bonds between water molecules and carboxylic oxygen atoms.

NMR Investigations of the Diamagnetic [Y$_2$(OHEC)]$^{2-}$ Complex

The lanthanide metals in the oxidation state Ln^{3+} are known to form stable but highly fluxional chelates with a variety of ligands.[6d] Their complexes with DOTA or with modified DOTA ligands together with a number of other O- or N-donor polydentate ligands[17] are among the very few examples exhibiting the same structure in the solid state as in solution. They form highly symmetric and extremely rigid structures, since the DOTA 12-membered tetraazacycle prefers to adopt a square {3 3 3 3} geometry offering a high degree of preorganisation.[6a] This is also valid for lanthanide(III) complexes of TETA, in which the cyclic ligand shows a biangular {7 7} conformation.[4g,18]

Also the large macrocyclic ligand H$_8$OHEC surprisingly forms a dinuclear yttrium(III) complex that is rigid on the NMR time scale. This fact gives the possibility of gaining some insight into the coordination characteristics and the solution structure of the complexes described here, and also to investigate whether conformational isomers possibly slowly equilibrate.

Temperature-dependent solution NMR studies of the diamagnetic dinuclear lanthanum(III) OHEC complex were unrevealing. The ^{1}H-NMR spectra in D$_2$O at 300 and 600 MHz showed a series of broad overlapping resonances characteristic of fluxional behaviour. A ^{1}H-NMR spectrum at 600 MHz of [(La$_2$(OHEC)]$^{2-}$ is shown as Supporting Information.

Figure 4 presents the experimental and the simulated ^{1}H-NMR spectra of [Y$_2$(OHEC)]$^{2-}$ at 278 K. Starting from the

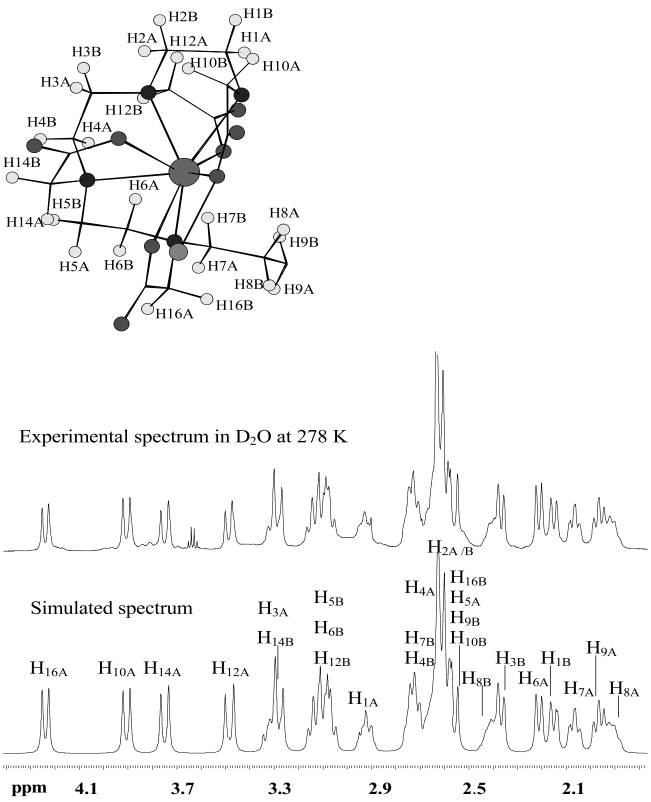

Figure 4. Experimental and simulated ^{1}H-NMR spectra of [Y$_2$(OHEC)]$^{2-}$ at 278 K in D$_2$O, pH = 8.5; plot of the asymmetric unit of [Y$_2$(OHEC)]$^{2-}$ illustrates the designation of atoms in the NMR spectra

Table 2. ^{1}H- and ^{13}C-NMR chemical shifts of Na$_2$[Y$_2$(OHEC)]

Backbone	protons	δ ^{1}H [ppm] at 278 K	δ ^{1}H [ppm] at 365 K	carbons	δ ^{13}C [ppm] at 278 K
N1	H1A	2.92	2.72	C1	57.4
	H1B	2.16	2.20		
	H2A	2.64	2.60	C2	53.4
	H2B	2.64	2.60		
N2	H3A	3.33	3.14	C3	53.9
	H3B	2.38	2.37		
	H4A	2.63	2.54	C4	52.5
	H4B	2.74	2.78		
N3	H5A	2.60	2.54	C5	54.3
	H5B	3.15	3.10		
	H6A	2.22	2.18	C6	47.5
	H6B	3.09	3.04		
N4	H7A	2.08	2.02	C7	55.7
	H7B	2.76	2.69		
	H8A	1.92	1.84	C8	19.8
	H8B	2.41	2.28		
	H9A	1.97	1.92	C9	55.9
	H9B	2.66	2.71		
side chain					
N1	H10A	3.91	3.78	C10	56.0
	H10B	2.56	2.55		
				C11	178.8
N2	H12A	3.49	3.51	C12	63.5
	H12B	3.11	3.01		
				C13	177.7
N3	H14A	3.26	3.31	C14	57.4
	H14B	3.76	3.53		
				C15	178.6
N4	H16A	4.25	4.15	C16	60.3
	H16B	2.61	2.59		
				C17	177.4

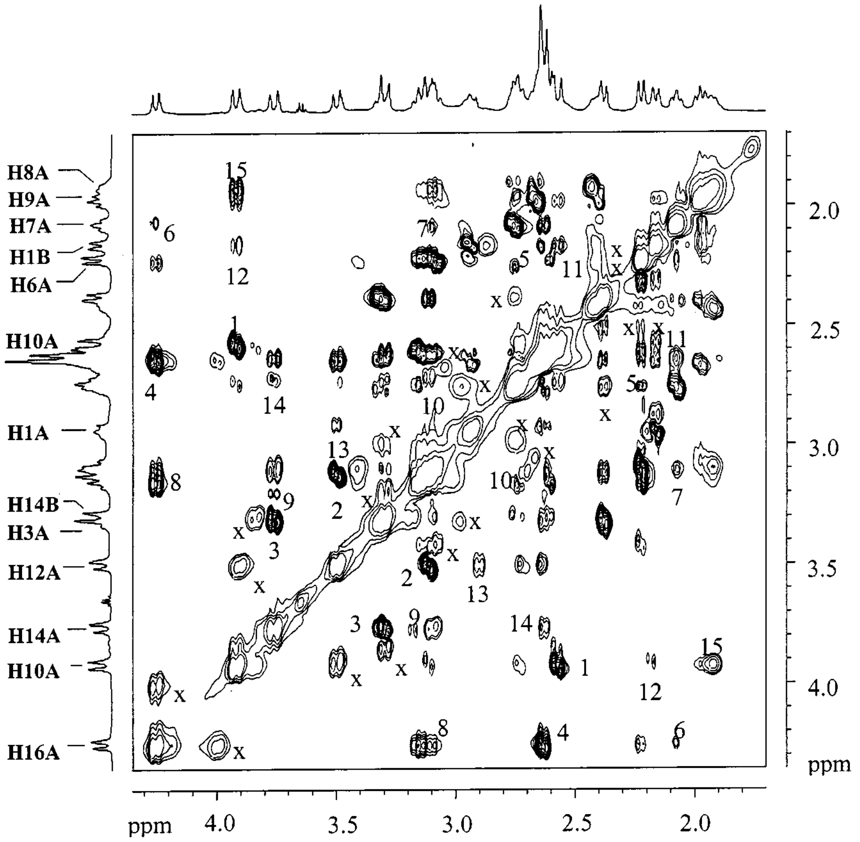

Figure 5. ROESY spectrum of $[Y_2(OHEC)]^{2-}$ at 278 K, mixing time 80 ms; the designation of the peaks is according to Table 3, column 4; exchange peaks are labelled with "x"

methylene proton H16A the step by step assignment was carried out with the HMQC and HMBC spectra and the cross peaks of the ROESY spectra. The ^1H- and ^{13}C chemical shift values are listed in Table 2 according to the designation in the solid-state structure.

Two features of these spectra are of particular interest. First, according to the centrosymmetric geometry of the complex in the solid state only half of the carbon and proton signals should appear in the NMR spectra. This is exactly the case for $[Y_2(OHEC)]^{2-}$, the solid-state geometry of which accounts for 26 proton and 17 carbon resonances, which all are observed in the spectra.

The second important feature of the ^1H-NMR spectrum (Figure 4) is the fact that the experimental spectrum clearly shows a few low intensity peaks indicating that at least two isomers (3.5:1 ratio) are present in aqueous solution. The minor isomer shows the signal number of an unsymmetric molecule, since temperature increase causes coalescence of each of the signals of the major conformation with two signals of the minor conformation. This loss of centrosymmetry may be caused by independent dynamic processes occurring in the two halves of the originally centrosymmetric molecule. Unfortunately, the NMR data do not allow an unambiguous assignment of the geometry of this minor isomer present in solution.

In order to determine the solution structure of $[Y_2(OHEC)]^{2-}$ a quantitative analysis of the ROESY spectra (Figure 5) measured at different mixing times was carried out. The intensity of the ROE signals was determined by measuring the volume of the ROESY cross peaks. On the basis of the X-ray crystal structure determination, the occurrence of non-sequential ROEs should be limited owing to the relatively large diameter of the complexed ligand. Hence, ROE information was only obtained from geminal

Table 3. Comparison of proton-proton distances derived from crystal structure and ROESY spectra

Proton pair		distance from crystal structur analysis [pm]	distance from ROE [pm]	No. in Figure 5
geminal protons				
H10A	H10B	156	170	1
H12A	H12B	157	170	2
H14A	H14B	156	170	3
H16A	H16B	157	160	4
Nongeminal protons				
H7B	H6A	212	240	5
H7A	H16A	259	270	6
H7A	H6B	226	220	7
H6B	H16A	235	210	8
H5B	H14B	270	270	9
H5B	H4B	240	220	10
H10B	H1B	253	260	11
H10A	H1B	245	270	12
H12A	H1A	246	240	13
H14B	H4B	215	240	14
H10A	H9A	202	190	15

protons and protons in close neighbourhood. Table 3 lists distances derived from the crystal structure and quantitative ROE measurements. The good agreement of the distance information obtained by these two different methods allows a strong resemblance to be claimed between solid and solution structure. The level of convergence of the structures was quantified by root mean square (rms) deviations calculated as the average of all possible pairwise comparisons, giving 50 ± 5 pm for comparisons based on all heavy atoms.

The low-temperature ROESY spectrum in Figure 5 proves the existence of an exchange process between major and minor conformation by the observation of exchange peaks, designated with ”x”, of protons undergoing mutual chemical exchange. All NMR signals of the major isomer show two exchange peaks at low temperatures.

For the methylene proton 16A of the acetate side arm, which is little disturbed by signal overlapping, variable-temperature ^{1}H-NMR spectra have been recorded and simulated (Figure 6). At 278 K the proton shows a doublet with an intensity of 78% for the major isomer, and two further doublets at higher field each with 11% of intensity for the minor isomer. With increasing temperature broadening and coalescence of the three signals occurs, followed by a sharpening to one doublet around 365 K. The band shapes of the depicted spectra were calculated for a two-site exchange. The kinetic parameters were deduced from the Arrhenius plot ($E_A = 51.3 \pm 2$ kJ/mol) and the Eyring plot ($\Delta H^{\#} = 49 \pm 2$ kJ/mol). The free energy of activation $\Delta G^{\#}$ at 300 K was calculated from the Eyring equation to be 65.0 ± 3 kJ/mol.

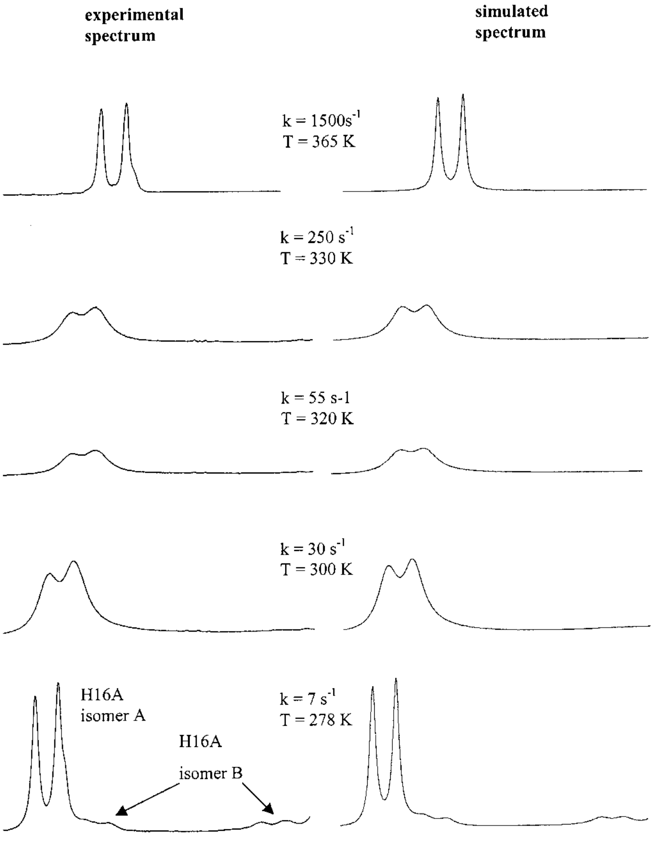

Figure 6. Selected experimental (on the left) and calculated (on the right) ^{1}H-NMR spectra of $[Y_2(OHEC)]^{2-}$ (CH_2 acetate region, proton H16A exchanging between two conformational environments) at different temperatures showing the derived rate constants

By comparison with the solution dynamics of the DOTA lanthanide complexes, two different types of motion should be possible within the $[Y_2(OHEC)]^{2-}$ moiety, one involving the rotation of the acetate arms and the other corresponding to a conformational inversion of the macrocyclic ring. Both processes potentially lead to an interchange between conformational isomers.[6] Although the DOTA and TETA complexes have totally different geometries the similar activation parameters of $[Y_2(OHEC)]^{2-}$ suggest a turning round of acetate groups without releasing the coordinative bonds.[6a,6d,4e,18]

Experimental Section

General Remarks: Materials: All reagents were purchased from Merck or Aldrich and were used without further purification. The ligand H_8OHEC as well as its yttrium(III) and lanthanide(III) complexes (Ln = Gd, Eu) were prepared by the published method.[9] – Elemental analyses and FAB mass spectra confirmed the composition of the compounds. The elemental analyses were recalculated for anhydrous compounds. The complexes contain at least two molecules of water per molecule of complex, dependent of the duration of the drying procedure. – Elemental analysis: Perkin–Elmer 2400 Series CHNS/O Analyzer. – MS: Double-focusing ZAB instrument, VG company (FAB).

H_8OHEC: M.p: 230–235°C. – $C_{34}H_{60}N_8O_{16}$ (836.41): calcd. C 48.80, H 7.23, N 13.39; found C 49.01, H 7.44, N 13.43%. – FAB$^+$MS (magic bullet/H_2O) *m/e*: 837 $[M + H]^+$, 859 $[M + Na]^+$, 875 $[M + K]^+$. Na^+ and K^+ are from impurities of the water used.

$Na_2[Y_2(OHEC)]$ (1): Dec. > 300°C. – $C_{34}H_{52}N_8Na_2O_{16}Y_2$ (1052.46): calcd. C 38.79, H 4.98, N 10.64; found C 38.60, H 4.69, N 10.38%.

$Na_2[Gd_2(OHEC)]$ (2): Dec. > 300°C. – $C_{34}H_{52}Gd_2N_8Na_2O_{16}$ (1189.25): calcd. C 34.34, H 4.41, N 9.42; found C 34.60, H 4.41, N 9.08%. – FAB$^+$MS of the complex (thioglycerine/methanol/H_2O) *m/e*: 1185–1196 $[M + H]^+$.

$Na_2[Eu_2(OHEC)]$ (3): Dec. > 300°C. – $C_{34}H_{52}Eu_2N_8Na_2O_{16}$ (1180.17): calcd. C 34.57, H 4.44, N 9.49; found C 34.83, H 4.53, N 10.00%. – FAB$^+$MS (thioglycerine/methanol/H_2O) *m/e*: 1177–1183 $[M + H]^+$.

$Cs_2[La_2(OHEC)]$ (4): The complex was prepared by treating 0.5 g (0.62 mmol) of H_8OHEC and 404.0 mg (1.24 mmol) of La_2O_3 suspended in 40 mL of distilled water. The mixture was refluxed for 24 h to obtain a clear solution. After cooling to room temperature and adjustment of the pH to 8.5 with 0.1 M Cs_2CO_3, the solution was refluxed for another 2 h and then filtered to remove traces of precipitated $La(OH)_3$. After removal of the solvent, the residue was recrystallised from water/ethanol. The separated colourless crystals were dried in vacuo at 80°C. Yield 76%. – $C_{34}H_{52}Cs_2La_2N_8O_{16}$ (1371.97): calcd. C 29.75, H 3.81, N 8.16; found C 29.53, H 4.01, N 8.08%. – FAB$^+$MS (thioglycerine/methanol/H_2O) *m/e*: 1394.5–1397.5 $[M + Na]^+$, 1128.8 $[M - 2 Cs+Na]^-$.

X-ray Crystallographic Study: Suitable crystals of **1** were obtained by slow diffusion of ethanol into a concentrated aqueous solution of the recrystallised diyttrium complex. Suitable crystals of **2**, **3**,

Table 4. Crystal data, details of data collection, and structure refinement for **1**, **2**, **3**, and **4**

	1	**2**	**3**	**4**
Crystal Data				
Empirical formula	$C_{34}H_{52}N_8Na_2O_{16}Y_2 \cdot 7\,H_2O \cdot C_2H_5OH$	$C_{34}H_{52}Gd_2N_8Na_2O_{16} \cdot 12\,H_2O$	$C_{34}H_{52}Eu_2N_8Na_2O_{16} \cdot 11\,H_2O$	$C_{34}H_{52}Cs_2La_2N_8O_{16} \cdot 14\,H_2O$
M_r [amu]	1242.81	1405.49	1412.94	1624.70
Crystal system	monoclinic	monoclinic	monoclinic	monoclinic
Space group	$P\,2_1/n$ (14)	$P\,2_1/n$ (14)	$P\,2_1$ /n (14)	$P\,2_1$ /n (14)
Crystal size [mm]	0.56 × 0.48 × 0.28	0.40 × 0.32 × 0.20	0.72 × 0.64 × 0.20	0.39 × 0.32 × 0.12
a [pm]	1481.8 (2)	1380.6 (2)	1394.3 (4)	1241.2 (2)
b [pm]	1224.0 (2)	2654.5 (3)	2673.5 (6)	1404.7 (2)
c [pm]	1572.9 (3)	1478.5 (2)	1485.2 (5)	1721.9 (3)
α [°]	90	90	90	90
β [°]	112.42 (2)	107.09 (2)	106.97 (3)	110.70 (2)
γ [°]	90	90	90	90
V [Å ^{3}]	2637.2 (6)	5178.9 (11)	5295 (3)	2808.4 (8)
ρ_{calc} [gcm^{-3}]	1.595	1.849	1.772	1.921
Z	2	4	4	2
F (000) [e]	600	1608	2872	1608
μ (Mo-$K\alpha$) [mm^{-1}]	2.299	2.657	2.46	2.872
Data Collection				
Diffractometer	STOE Ipds	STOE Ipds	STOE Stadi-4	STOE Ipds
Radiation, [Å]		Mo Kα, 0.71071	graphite monochromator	
T [K]	200 (2)	200 (2)	295 (2)	200 (2)
scan mode	φ - rotation	φ - rotation	2Θ/ω = 0.5	φ - oscillation
h, k, l ranges	±10, ±10, ±13	−16/15, ±31, ± 17	−16/15, 0/31, −16/17	−15/14, ±17, ±20
2Θ range [°]	4.46−47.0	3.86−50.22	3.04−49.98	4.56−50.24
Measured data	11802	34400	10459	18680
unique data (all)	3904	9041	9259	5023
R_{int}	0.1096	0.0920	0.0631	0.1709
data used f. refinement	3904	9040	9235	5011
Absorption correction	refdelf (difabs)	refdelf (difabs)	empirical (ψ -scan)	no
T_{min}/T_{max}	0.447/1.0	0.523/0.998	0.548/0.997	−/−
Refinement				
refined parameters	435	763	674	343
H atoms [found/geom.]	32/0	24/52	24/52	10/26
$R1$[a] [$F_0 > 4\sigma(F_0)$]	0.0300 (2966 refl.)	0.0307 (7482)	0.0432 (7751)	0.0556 (3684)
$wR2$[b] (all)	0.0935	0.0818	0.1188	0.1434
GoF (all)	0.912	0.991	1.141	0.976
Weighting par.a,b[c]	0.0371, 0	0.0381, 0	0.048, 0.0098	0.0597, 0
ρ_{final}(max/min) [e Å $^{-3}$]	0.542/−0.659	2.172/−0.832	2.872/−1.027	3.464/−1.531

[a] $R1 = \Sigma||F_o| - |F_c||/\Sigma|F_o|$. − [b] $wR2 = [\Sigma\, w(F_o^2 - F_c^2)^2/\Sigma\, w(F_o^2)^2]^{1/2}$. − [c] $w = 1/[\sigma^2(F_o^2) + (a\,P)^2 + b\,P]$; $P = (F_o^2 + 2F_c^2)/3$.

and **4** were obtained by slow evaporation of a concentrated aqueous solution of the recrystallised dilanthanide complexes.

The single crystals of compounds **1**, **2**, and **4** were measured on the STOE Ipds one circle diffractometer supplied with an imaging plate area detector at 200 K in nitrogen atmosphere. Intensity correction for Lorentz and polarisation effects and in the case of **1** and **2** also for absorption (Difabs-related)[19] was applied.

A crystal of the compound **3** was measured on a STOE Stadi-4 four circle diffractometer at room temperature in air. Intensity data were corrected for Lorentz, polarisation and absorption (ψ-scan technique).[20]

Structures were solved by direct methods[21] and refined by full-matrix least squares against F^2[22] supported by STOE Xstep software. The thermal motion of all non-hydrogen atoms was treated anisotropically, that of hydrogen atoms isotropically and tied 1.2 times higher than the corresponding attached atom.

In the structure of **1** the positions of all H-atoms of the OHEC unit and six H-positions of water molecules were found in difference electron density maps (difmaps) and successfully refined in least-squares refinement. The H-atoms at the partially occupied water and ethanol sites could not be localised.

For the refinement of **2**, **3**, and **4** the hydrogen atoms of the OHEC units were calculated in their idealised positions and allowed to ride on their attached atoms during the least squares cycles.

In structure **2** two of fourteen water positions have site occupation factors of only 0.8 and 0.5. All H atoms at fully occupied water sites were found in difmaps and their positions could be refined by least squares.

In structure **3**, where either two of fourteen water sites are not fully occupied (0.67 and 0.33 in part, respectively), all H atoms of fully occupied water sites were localised in difmaps, but had to be fixed in the following least squares cycles.

In the crystal structure of **4** all seven water sites are completely occupied, but nevertheless only ten of fourteen water hydrogens could be found in difmaps (obviously the data set of **4** was of poor quality; even the application of difabs failed!). Consequently, all hydrogen atoms had to be restrained or fixed for least-squares refinement.

Further details of the crystal-structure investigations may be obtained from the Fachinformationszentrum Karlsruhe, D-76344 Eggenstein- Leopoldshafen, Germany, on quoting the depository numbers CSD-410446 for **1**, CSD-410447 for **2**, CSD-410444 for **3**, and CSD-410445 for **4**.

NMR: Samples for NMR spectroscopy were prepared by dissolving 50 mg of the complex in 0.75 mL of D_2O in a 5-mm sample tube (Wilmad). NMR spectra were acquired at 600 MHz on a Bruker AMX 600 spectrometer. 2D spectra (DQF-COSY, ROESY, TOCSY, HSQC, and HMBC) were recorded at 278 K with a spectral width of 7200 Hz for protons and 33000 Hz for ^{13}C. The TPPI method of acquisition was used in all cases. The signal due to residual HDO was suppressed by continuous low-power irradiation. Data matrices typically consisted of 2048 complex points in F2 for each of the 512 F1 increments, the data being zero-filled to a 2048 × 1024 complex matrix before transformation. The apodisation functions used in processing were 90° shifted sine-bell squared for all 2D experiments. 2D spectra were processed using the UXNMR program on a Silicon Graphics O2 workstation. ROESY crosspeaks were integrated by the AURELIA[23] software including offset correction according to Bull.[24] The temperature dependence of the proton resonances was determined by recording the 1D spectra at 278 to 373 K with temperature steps of 10 K. The temperature was calibrated against a 100% ethylene glycol insert sample. Rate constants were evaluated by comparing the experimental spectra with those calculated with the program DNMR-SIM.[25] The simulation of one dimensional ^{1}H-NMR spectra were performed with the Bruker Software WIN-DAISY.[26]

Acknowledgments

This work was supported by the *Fonds der Chemischen Industrie* and the *Deutsche Forschungsgemeinschaft* as well as the Sonderforschungsbereich 335 Anisotrope Fluide.

---

[1] V. Alexander, *Chem. Rev.* **1995**, *95*, 273−342.

[2] [2a] J. P. L. Cox, K. J. Jankowski, R. Kataky, D. Parker, N. R. A. Beeley, B. A. Boyce, M. A. W. Eaton, K. Millar, A. T. Millican, A. Harrison, C. Walker, *J. Chem. Soc., Chem. Commun.* **1989**, 797−798. − [2b] D. Parker, *Crown Compounds Toward Future Applications* (Ed.: S.R. Cooper), VCH Publishers, Inc., New York, **1992**, Chapter 4.

[3] [3a] R. B. Lauffer, *Chem. Rev.* **1987**, *87*, 901−927. − [3b] R. G. Choppin, K. M. Schaab, *Inorg. Chim. Acta* **1996**, *252*, 299−310.

[4] [4a] M.-R. Spirlet, J. Rebizant, J. F. Desreux, M.-F. Loncin, *Inorg. Chem.* **1984**, *23*, 359−363. − [4b] J. P. Dubost, J. M. Legar, M. H. Langlois, D. Meyer, M. C. R. Schaefer, *Acad. Sci. Paris Ser. 2* **1991**, *312*, 349. − [4c] C. A. Chang, L. C. Francesconi, M. F. Malley, K. Kumar, J. Z. Gougoutas, M. F. Tweedle, *Inorg. Chem.* **1993**, 32, 3501−3508. − [4d] D. Parker, K. Pulukkody, F. C. Smith, A. Batsanov, J. A. K. Howard, *J. Chem. Soc. Dalton Trans.* **1994**, 689−693. − [4e] S. Aime, A. Barge, M. Botta, M. Fasano, J. D. Ayala, G. Bombieri, *Inorg. Chim. Acta* **1996**, *246*, 423−429. − [4f] S. Aime, A. Barge, F. Benetello, G. Bombieri, M. Botta, F. Uggeri, *Inorg. Chem.* **1997**, *36*, 4287−4289. − [4g] M.-R. Spirlet, J. Rebizant, M. F. Loncin, J. F. Desreux, *Inorg. Chem.* **1984**, *23*, 4278−4283.

[5] [5a] S. Aime, P. L. Anelli, M. Botta, F. Fedeli, M. Grandi, P. Paoli, F. Uggeri, *Inorg. Chem.* **1992**, *31*, 2422−2428. − [5b] S. Aime, M. Botta, G. Ermondi, F. Fedeli, F. Uggeri, *Inorg. Chem.* **1992**, *31*, 1100−1103. − [5c] D. Dischino, E. J. Delaney, J. E. Emswiler, G. T. Gaughan, J. S. Prasad, S. K. Srivastava, M. F. Tweedle, *Inorg. Chem.* **1991**, *30*, 1265−1269. − [5d] S. I. Kang, R. S. Ranganathan, J. E. Emswiler, K. Kumar, J. Z. Gougoutas, M. F. Malley, M. F. Tweedle, *Inorg. Chem.* **1993**, *32*, 2912−2918. − [5e] K. Kumar, C. A. Chang, L. C. Francesconi, D. D. Dischino, M. F. Malley, M. F. Gougoutas, M. F. Tweedle, *Inorg. Chem.* **1994**, *33*, 3567−3575. − [5f] Z. Kovacs, A. D. Sherry, *J. Chem. Soc., Chem.Commun.* 1995, 185−186. − [5g] J. Huskens, D. A. Torres, Z. Kovacs, J. P. André, C. F. G. C. Geraldes, A. D. Sherry, *Inorg. Chem.* **1997**, *36*, 1495−1503. − [5h] J. Platzek, P. Blaszkiewicz, H. Gries, P. Luger, G. Michl, A. Müller- Fahrnow, B. Radüchel, D. Sülzle, *Inorg. Chem.* **1997**, *36*, 6086−6093.

[6] [6a] J. F. Desreux, *Inorg. Chem.* **1980**, *19*, 1319−1324. − [6b] S. Aime, M. Botta, G. Ermondi, *Inorg. Chem.* **1992**, *31*, 4291−4299. − [6c] K. Roth, S. Hoeft, *Chem. Ber.* **1993**, *126*, 869−873. − [6d] V. Jacques, J. F. Desreux, *Inorg. Chem.* **1994**, *33*, 4048−4053. − [6e] S. Aime, M. Botta, M. Fasano, P. M. Marques, C. F. G. C. Geraldes, D. Pubanz, A. E. Merbach, *Inorg. Chem.* **1997**, *36*, 2059−2068 and references cited therein. − [6f] S. Aime, M. Botta, G. Ermondi, E. Terreno, P. L. Anelli, F. Fedeli, F. Uggeri, *Inorg. Chem.* **1996**, *35*, 2726−2736. − [6g] S. Aime, M. Botta, A. S. De Sousa, D. Parker, *Angew. Chem.* **1998**, *110*, 2819−2820.

[7] R. Ziessel, M. Maestri, L. Pridi, V. Balzani, A. V. Dorsselaer, *Inorg. Chem.* **1993**, *32*, 1237−1241.

[8] E. Tóth, S. Vauthey, D. Pubanz, A. E. Merbach, *Inorg. Chem.* **1996**, *35*, 3375−3379.

[9] U. A. Böttger, H. Gries, F. E. Hahn, H. Hemling, G. Kociok-Köhn, J. Pickardt, J. Platzek, B. Radüchel, B. Schiefner, H. Schumann, K. Zietzke, A. Zschunke, *Chem. Ber.* **1997**, *130*, 267−277.

[10] U. A. Böttger, H. Weisshoff, A. Zschunke, H. Schumann, to be published.

[11] [11a] M. Kodama, T Koike, A. B. Mahatma, E. Kimura, *Inorg. Chem.* **1991**, *30*, 1270−1273. − [11b] S. L. Wu, W. D. Horrocks, Jr., *Inorg. Chem.* **1995**, *34*, 3724−3732.

[12] S. L. Wu, K. A. Johnson, W. D. Horrocks, Jr., *Inorg. Chem.* **1997**, *36*, 1884−1889.

[13] C. Lecomte, V. Dahaoui-Gindrey, H. Chollet, C. Gros, A. K. Mishra, F. Barbette, P. Pullumbi, R. Guilard, *Inorg. Chem.* **1997**, *36*, 3827−3838.

[14] U. Böttger, O. Galin, H. Schumann, M. Michman, *Inorg. Chim. Acta* **1995**, *231*, 29−34.

[15] M. G. B. Drew, *Coord. Chem. Rev.* **1977**, *24*, 179−275 and references cited therein.

[16] J. Dale, *Isr. J. Chem.* **1980**, *20*, 3−11.

[17] [17a] P. M. Lowe, P. Caravan, S. J. Rettig, C. Orvig, *Inorg. Chem.*, **1998**, *37*, 1637−1647. − [17b] F. Renaud, C. Piguet, G. Bernardinelli, J.-C. G. Bünzli, G. Hopfgartner, *Chem. Eur. J.*, **1997**, *3*, 1646−1659.

[18] J. F. Desreux, M. F. Loncin, *Inorg. Chem.* **1986**, *25*, 69−74.

[19] N. Walker, D. Stuart, *Acta Cryst. A39* **1983**, 158−166.

[20] A. C. T. North, D. C. Phillips, F. S. Mathews, *Acta Cryst. A24* **1968**, 351−359.

[21] G. M. Sheldrick, *Acta Cryst. A46* **1990**, 467−473.

[22] G. M. Sheldrick, *Program for Crystal Structure Refinement* **1993**, Universität Göttingen, Germany.

[23] *AURELIA* manual, version 941101.3 Bruker Analytische Messtechnik GmbH, FRG, **1994**.

[24] T. E. J. Bull, *Magn. Reson.***1988**, *80*, 470.

[25] *DNMR-SIM*, version 1.00, G. Haegele, R. Fuhler, Institut für Anorganische und Strukturchemie I, Universität Düsseldorf, FRG, **1996**. This program is available on the Internet: ftp://ftp.uni-duesseldorf.de/pub/msdos/chemie.

[26] WIN-DAISY, version 4.0 Bruker-Franzen Analytik GmbH, FRG, **1997**.

Received March 3, 1999
[I99081]